

See discussions, stats, and author profiles for this publication at: <https://www.researchgate.net/publication/231238113>

Structure of Exfoliated Titanate Nanosheets Determined by Atomic Pair Distribution Function Analysis

ARTICLE *in* CHEMISTRY OF MATERIALS · NOVEMBER 2004

Impact Factor: 8.35 · DOI: 10.1021/cm0488884

CITATIONS

21

READS

31

5 AUTHORS, INCLUDING:



Yang Ren

Argonne National Laboratory

488 PUBLICATIONS 6,231 CITATIONS

SEE PROFILE



Valeri Petkov

Central Michigan University

66 PUBLICATIONS 1,343 CITATIONS

SEE PROFILE

Structure of Exfoliated Titanate Nanosheets Determined by Atomic Pair Distribution Function Analysis

Milen Gateshki,[†] Seong-Ju Hwang,[‡] Dae Hoon Park,[‡] Yang Ren,[§] and Valeri Petkov^{*,†}

Department of Physics, Central Michigan University, 203 Dow Science, Mt. Pleasant, Michigan 48859, Department of Applied Chemistry, Center for Optoelectronic and Microwave Devices, College of Natural Sciences, Konkuk University Chungju Campus, Chungbuk 380-701, Korea, and Advanced Photon Source, Argonne National Laboratory, Argonne, Illinois 60439

Received July 8, 2004. Revised Manuscript Received September 13, 2004

Colloidal suspension of titanate nanosheets has been prepared by exfoliation of $\text{Cs}_{0.67}\text{Ti}_{1.83}\text{O}_4$ through the intercalation of tetrabutylammonium (TBA). The atomic scale structure of the nanosheets has been determined using X-ray diffraction and the atomic pair distribution function (PDF) technique. The exfoliated titanate nanosheets have been found to be an irregular assembly of double layers of $\text{Ti}-\text{O}_6$ octahedra accommodating water and TBA molecules in the interlayer space. The interlayer distances show a wide distribution ranging from 9 to at least 18 Å. The separation between the titanate layers remains nearly the same in air-dried product of the colloidal suspension.

Introduction

The exfoliation of cesium titanate is currently a subject of increasing interest since it can provide a colloidal suspension of titanate nanosheets.^{1–11} Such a colloidal suspension has been used as a precursor for the fabrication of ultrathin hollow shells with diameters in the micrometer range,¹ mesoporous metal oxide sol pillared nanohybrids,^{3,4} and also titanate and multilayer heterostructure thin films.^{5,6} From a fundamental point of view, layered titanates are considered as good model structures for the study of processes such as exfoliation, delamination, and osmotic swelling.^{9,10} Previous structure studies on titanate nanosheets have concentrated either on the starting layered titanate materials,³ or on the dried restacked product.⁴ However, almost all applications of titanate nanosheets involve their colloidal suspension. Experiments on nanosheets suspended in

water have also been carried out^{9,10} but they have been aimed mostly at revealing the relative arrangement of the exfoliated nanosheets and not on their atomic-scale structure. Information about the 3D atomic ordering in the nanosheets is important for better understanding of the useful material's properties. In the present paper we report results from structure studies on colloidal suspension of $\text{Ti}_{1.83}\text{O}_4$ nanosheets performed by the atomic pair distribution function (PDF) technique, which is known to be well-suited for materials showing limited structural coherence.

Experimental Section

Sample Preparation. The precursor cesium titanate, $\text{Cs}_{0.67}\text{Ti}_{1.83}\text{O}_4$, was prepared by heating a mixture of Cs_2CO_3 and TiO_2 at 800 °C for 20 h. The corresponding protonic form, $\text{H}_{0.67}\text{Ti}_{1.83}\text{O}_4$, was obtained by reacting cesium titanate powder with 1 M HCl aqueous solution at room temperature for 3 days. During this proton exchange reaction, the HCl solution was replaced with fresh solution every day. The exfoliation of cesium titanate lattice was achieved by reacting the protonic titanate with tetrabutylammonium hydroxide (TBA·OH) for more than 2 weeks. For an effective exfoliation, the amount of TBA·OH was adjusted to be equivalent to that of the exchangeable protons in $\text{H}_{0.67}\text{Ti}_{1.83}\text{O}_4\cdot\text{H}_2\text{O}$. After the reaction, a small amount of incompletely exfoliated particles was removed through centrifugation at a speed of 12 000 rpm for 10 min. For XRD measurement, a dense suspension of wet titanate nanoparticles was prepared by applying an additional centrifugation under extreme condition (18 000 rpm for 1 h).

X-ray Diffraction Experiments. XRD experiments on the suspension of wet titanate nanoparticles and the solid parent material $\text{Cs}_{0.67}\text{Ti}_{1.83}\text{O}_4$ were carried out at the beamline 11-ID-C (Advanced Photon Source, Argonne National Laboratory) using X-rays of energy 115.013 keV ($\lambda = 0.1078$ Å). The higher energy X-rays were used to extend the region of reciprocal space covered (i.e., to obtain data at higher wave vectors, Q) which is important for the success of PDF analysis. Special care was taken to maintain the wet state of the exfoliated

* To whom all correspondence should be addressed. E-mail: petkov@phy.cmich.edu.

[†] Central Michigan University.

[‡] Konkuk University.

[§] Argonne National Laboratory.

(1) Wang, L.; Sasaki, T.; Ebina, Y.; Kurashima, K.; Watanabe, M. *Chem. Mater.* **2002**, *14*, 4827.

(2) Fukuda, K.; Sasaki, T.; Watanabe, M.; Nakai, I.; Inaba, K.; Omote, K. *Cryst. Growth Des.* **2003**, *3*, 281.

(3) Choy, J.-H.; Lee, H.-C.; Jung, H.; Hwang, S.-J. *J. Mater. Chem.* **2001**, *11*, 2232.

(4) Kooli, F.; Sasaki, T.; Rives, V.; Watanabe, M. *J. Mater. Chem.* **2000**, *10*, 497.

(5) Sasaki, T.; Ebina, Y.; Tanaka, T.; Harada, M.; Watanabe, M. *Chem. Mater.* **2001**, *13*, 4661.

(6) Wang, Z. S.; Sasaki, T.; Muramatsu, M.; Ebina, Y.; Tanaka, T.; Wang, L.; Watanabe, M. *Chem. Mater.* **2003**, *15*, 807.

(7) Sasaki, T.; Ebina, Y.; Watanabe, M.; Decher, G. *Chem. Commun.* **2000**, 2163.

(8) Sasaki, T.; Ebina, Y.; Kitami, Y. M.; Watanabe, M.; Oikawa, T. *J. Phys. Chem. B* **2001**, *105*, 6116.

(9) Sasaki, T.; Watanabe, M. *J. Am. Chem. Soc.* **1998**, *120*, 4682.

(10) Sasaki, T.; Watanabe, M.; Hashizume, H.; Yamada, H.; Nakazawa, H. *J. Am. Chem. Soc.* **1996**, *118*, 8329.

(11) Sasaki, T.; Watanabe, M. *J. Phys. Chem. B* **1997**, *101*, 10159.

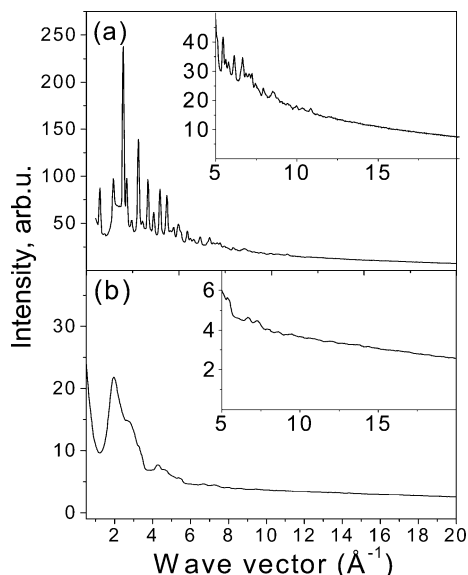


Figure 1. Experimental diffraction patterns of (a) crystalline $\text{Cs}_{0.67}\text{Ti}_{1.83}\text{O}_4$ and (b) the suspension of exfoliated titanate nanosheets. The higher- Q portion of the patterns is given on an enlarged scale in the insets.

titanate suspension by sealing the samples between Capton foils. The measurements were carried out in symmetric transmission geometry and scattered radiation was collected with an intrinsic germanium detector connected to a multi-channel analyzer. Several runs were conducted with each of the samples and the resulting XRD patterns were averaged to improve the statistical accuracy and reduce any systematic effect due to instabilities in the experimental setup. The diffraction patterns obtained are shown in Figure 1. As can be seen, the XRD pattern of $\text{Cs}_{0.67}\text{Ti}_{1.83}\text{O}_4$ exhibits well-defined Bragg peaks up to $Q \approx 12 \text{ \AA}^{-1}$.

The material is obviously perfectly crystalline. The XRD pattern of the colloidal suspension of titanate nanosheets, on the other hand, shows only a few Bragg-like features and a pronounced, slowly oscillating diffuse component. The observed XRD pattern is in good agreement with the previously reported pattern of titanate colloidal suspension collected with $\text{Cu K}\alpha$ radiation.^{9,10} Such a diffraction pattern is practically impossible to be tackled by ordinary techniques for structure determination. However, once reduced to the corresponding atomic PDF, it becomes a structure-sensitive quantity lending itself to structure determination. The frequently used reduced atomic PDF, $G(r)$, is defined as follows:

$$G(r) = 4\pi r [\rho(r) - \rho_0] \quad (1)$$

where $\rho(r)$ and ρ_0 are the local and average atomic number densities, respectively, and r is the radial distance.¹² It peaks at characteristic distances separating pairs of atoms and thus reflects the atomic scale structure. The PDF $G(r)$ is the Fourier transform of the experimentally observable total structure function, $S(Q)$, i.e.,

$$G(r) = (2/\pi) \int_{Q=0}^{Q_{\max}} Q[S(Q) - 1] \sin(Qr) dQ \quad (2)$$

where Q is the magnitude of the wave vector ($Q = 4\pi \sin \theta / \lambda$), 2θ is the angle between the incoming and outgoing radiation beams and λ is the wavelength of the radiation used. The structure function is related to the coherent part of the total diffracted intensity as follows:

$$S(Q) = 1 + [I^{\text{coh}}(Q) - \sum c_i |f_i(Q)|^2] / \sum c_i f_i(Q)^2 \quad (3)$$

where $I^{\text{coh}}(Q)$ is the coherent scattering intensity per atom in electron units and c_i and f_i are the atomic concentration and

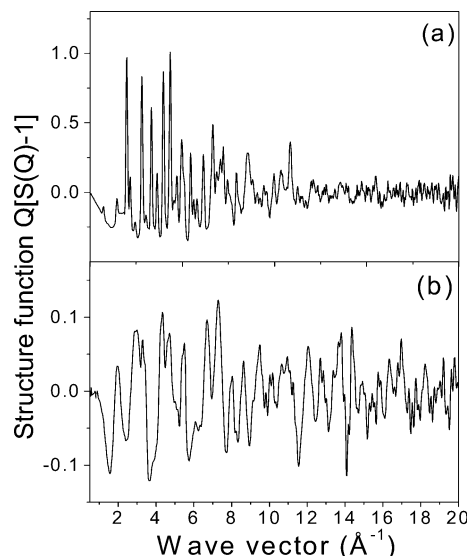


Figure 2. Experimental structure functions $Q[S(Q) - 1]$ for (a) crystalline $\text{Cs}_{0.67}\text{Ti}_{1.83}\text{O}_4$ and (b) the suspension of exfoliated titanate nanosheets as obtained from the diffraction patterns of Figure 1.

X-ray scattering factor, respectively, for the atomic species of type i . As can be seen from eqs 1–3, $G(r)$ is simply another representation of the powder diffraction data. However, exploring the diffraction data in real space is advantageous, especially in the case of materials with limited structural coherence. First, as eq 2 implies, the total scattering, including Bragg scattering as well as diffuse scattering, contributes to the PDF. In this way both the long-range atomic structure, manifested in the sharp Bragg peaks, and the local nonperiodic structural imperfections, manifested in the diffuse components of the diffraction pattern, are reflected in the PDF. Second, by accessing high values of Q , experimental $G(r)$ s with high real-space resolution can be obtained and hence, quite fine structural features can be revealed. In fact, data at high Q values ($Q > 10 \text{ \AA}^{-1}$) are critical to the success of PDF analysis. Third, $G(r)$ is less affected by diffraction optics and experimental factors since these are accounted for in the step of extracting the coherent intensities from the raw diffraction data. This renders the PDF a structure-dependent quantity giving directly relative positions of atoms in materials. As we have already demonstrated in several studies on nanocrystalline materials,^{13–15} this enables convenient testing and refinement of structural models.

Experimental PDFs for the studied samples were obtained as follows. First, the coherently scattered intensities were extracted from the XRD patterns of Figure 1 by applying appropriate corrections for flux, background, Compton scattering, and sample absorption. The intensities were normalized in absolute electron units and reduced to the structure functions $Q[S(Q) - 1]$ shown in Figure 2.

The structure functions were Fourier transformed to atomic PDFs according to eq 2. All data processing was done using the program RAD.¹⁶ Thus-obtained experimental PDFs are plotted in Figure 3.

As can be seen, the experimental PDF for crystalline $\text{Cs}_{0.67}\text{Ti}_{1.83}\text{O}_4$ is rich in well-defined structural features extending to high real-space distances, as it should be with a material possessing 3D periodicity and long-range atomic order. The

(12) Klug, H. P.; Alexander, L. E. *X-ray Diffraction Procedures for Polycrystalline Materials*; Wiley: New York, 1974.

(13) Petkov, V.; Billinge, S. J. L.; Larson, P.; Mahanti, S. D.; Vogt, T.; Rangan, K. K.; Kanatzidis, M. G. *Phys. Rev. B* **2002**, *65*, 092105.

(14) Petkov, V.; Trikalitis, P. N.; Bozin, E. S.; Billinge, S. J. L.; Vogt, T.; Kanatzidis, M. G. *J. Am. Chem. Soc.* **2002**, *124*, 10157.

(15) Petkov, V.; Zavalij, P. Y.; Lutta, S.; Whittingham, M. S.; Parvanov, V.; Shastri, S. *Phys. Rev. B* **2004**, *69*, 085410.

(16) Petkov, V. *J. Appl. Crystallogr.* **1989**, *22*, 387.

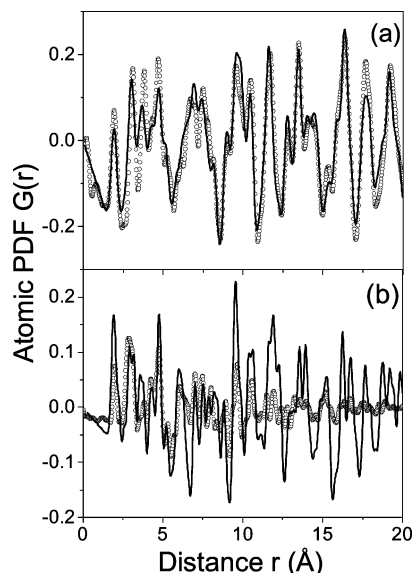


Figure 3. Experimental (symbols) and model (line) atomic PDFs $G(r)$ for (a) crystalline $\text{Cs}_{0.67}\text{Ti}_{1.83}\text{O}_4$ and (b) the suspension of exfoliated titanate nanosheets. The model data are computed on the basis of the crystal structure of cesium titanate¹⁷ and protonic titanate,¹⁹ respectively.

PDF for the colloidal suspension of titanate nanosheets is also rich in well-defined features but those features vanish already at 15–18 Å. Obviously, this nanocrystalline material has a very well-defined local atomic arrangement but lacks the extended order of usual crystals.

Results and Discussion

Even though the structure of crystalline $\text{Cs}_{0.67}\text{Ti}_{1.83}\text{O}_4$ is well-known, it was again studied here to test the quality of the present experimental data and illustrate the capabilities of the PDF technique. Like other techniques employed in structure determination of materials, the PDF method uses a least-squares procedure to compare experimental and model PDFs calculated from a plausible starting model. The structural parameters of the model are adjusted until the best fit to the experimental PDF data is achieved. Crystalline $\text{Cs}_{0.67}\text{Ti}_{1.83}\text{O}_4$ possesses an orthorhombic structure built of layers of edge-shared TiO_6 octahedral units with Cs atoms occupying the space between the layers,¹⁷ as shown in Figure 4.

Data from literature sources¹⁷ were used as initial values for the structural parameters of $\text{Cs}_{0.67}\text{Ti}_{1.83}\text{O}_4$. They were refined against the present PDF data observing the constraints of the *Immm* space group. The fit was done with the help of the program PDFFIT.¹⁸ It converged rapidly and produced a model PDF that reproduces the experimental one in detail as shown in Figure 3a. The refined structure parameters are summarized in Table 1. They agree very well with results from previous structure studies.¹⁷ This outcome of our study well demonstrates the good quality of the present experimental data and the ability of the PDF technique to reveal the atomic ordering in materials.

To determine the structure of titanate nanosheets we considered several trial models, as follows. At first, a

Table 1. Structural Parameters of $\text{Cs}_{0.67}\text{Ti}_{1.83}\text{O}_4$ at Room Temperature Obtained from PDF Refinement^a

atom	position	occupancy	<i>x</i>	<i>y</i>	<i>z</i>	<i>B</i> _{iso} (Å ²)
Cs	4i	0.335	0.0	0.0	0.182(5)	6.34(7)
Ti	4h	0.915	0.0	0.3078(2)	0.5	0.94(1)
O1	4g	1.0	0.0	0.2235(6)	0.0	2.08(1)
O2	4g	1.0	0.0	0.3752(5)	0.0	2.08(1)

^a Structural model has the *Immm* space group. *a* = 3.781(2) Å; *b* = 17.319(5) Å; *c* = 2.923(1) Å.

model based on the protonic titanate structure was considered. The protonic titanate is obtained at the first stage of the chemical route employed by us when Cs atoms are removed from the $\text{Cs}_{0.67}\text{Ti}_{1.83}\text{O}_4$ crystal and replaced by H^+ cations. As already discussed,¹⁹ the extraction of Cs results in the introduction of considerable structural disorder and profound smearing out of the Bragg diffraction peaks, something we observe in the diffraction pattern of titanate nanosheets (see Figure 1b). A model PDF calculated from the structure of protonic titanate¹⁹ is shown in Figure 3b. As can be seen in the figure, this model is not capable of reproducing the experimental data for the nanosheets. In particular, it gives many sharp peaks at *r* values higher than 9 Å reflecting the presence of a long-range ordered stack of double TiO_2 layers.¹⁹ This is not exactly the picture seen with exfoliated titanate sheets, as their PDF decays almost to zero at *r* values higher than 18 Å. To account for the very limited structural coherence in the titanate sheets, we modified the structure model by introducing structural disorder leading to a rapid decay of the model PDF data. The degree of the disorder was varied until the high-*r* behavior of the model data closely followed that of the experimental data. This was another structure-related parameter adjusted with the help of the program PDFFIT. Furthermore, we took into account the presence of water in the interlayer space by adding to the model data an appropriately weighed term based on experimental PDF data for water. This modification introduced minor changes to the model PDF data due to the low scattering power of water but we kept it in the model to make it more realistic. The thus-modified model features titanate double layers separated at approximately 9 Å with interlayer space occupied by water. A model PDF calculated on the basis of the model is shown in Figure 5a.

As can be seen, it reproduces all important details in the experimental data. Considering that the sample was made by a soft chemistry route and, therefore, possesses a high degree of disorder, the level of agreement achieved is quite good and acceptable. The only deficiency of the model is that it gives peaks that are somewhat sharper than the experimental ones at distances higher than 9 Å (see the peaks marked with arrows in Figure 5a). Since in our model correlations between neighboring layers begin to show up at distances longer than 9 Å one can conclude that the model somewhat overestimates the degree of order between the neighboring layers and/or underestimates their separation. This prompted us to investigate a model where the layers are separated at a longer distance, namely, 18 Å. The atomic coordinates of titanate layers in this model are listed in Table 2.

(17) Grey, I. E.; Li, C.; Madsen, I. C.; Watts, J. A. *J. Solid State Chem.* **1989**, *66*, 7.

(18) Proffen, Th.; Billinge, S. J. L. *J. Appl. Crystallogr.* **1999**, *32*, 572.

(19) Sasaki, T.; Watanabe, M.; Michiue, Y.; Komatsu, Y.; Izumu, F.; Takenouchi, S. *Chem. Mater.* **1995**, *7*, 1001.

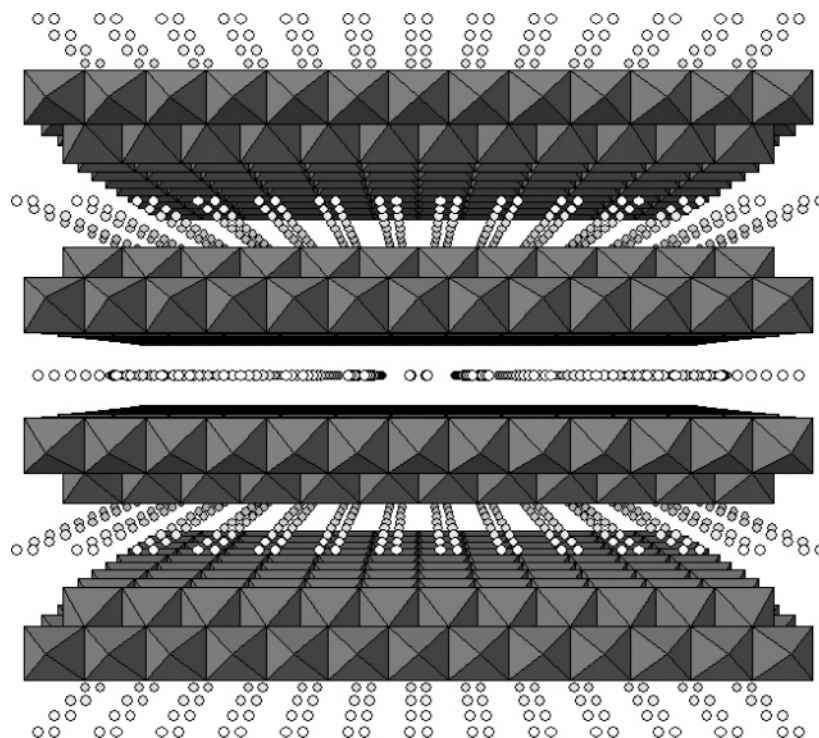


Figure 4. Polyhedral representation of the crystal structure of pristine $\text{Cs}_{0.67}\text{Ti}_{1.83}\text{O}_4$. The structure may be viewed as a stack of double layers of Ti–O₆ octahedra with Cs atoms (circles) alternating in the open space between the layers.

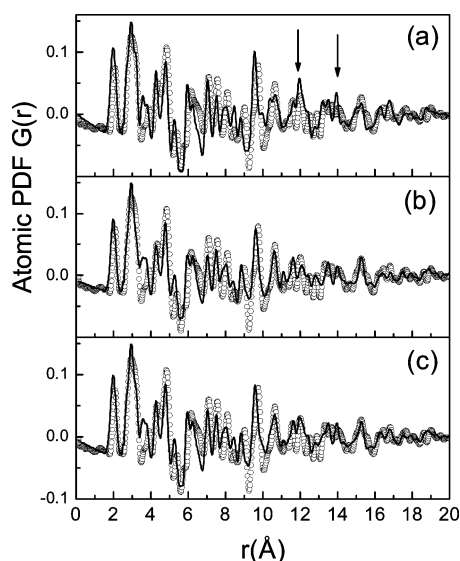


Figure 5. Experimental (symbols) and model (line) PDFs for exfoliated titanate nanosheets. (a) Model featuring double layers separated by approximately 9 Å. Correlations between neighboring layers show up at distances longer than 9 Å as marked with arrows. (b) Model featuring double layers separated by approximately 18 Å. (c) Model featuring two sets of double layers separated by 9 and 18 Å, respectively.

A PDF calculated on the basis of this model is shown in Figure 5b. For short interatomic distances it reproduces the experimental data as well as the model featuring layers separated at 9 Å. For longer real space distances (>9 Å) it follows the smooth behavior of the experimental data suggesting that 18 Å is a more realistic separation between the titanate layers in water. This outcome of our modeling studies is supported by the diffraction pattern of titanate nanosheets dried in air (Figure 6).

Table 2. Parameters of the Model Titanate Structure Used for Comparison with the Experimental Data^a

atom	position	occupancy	<i>x</i>	<i>y</i>	<i>z</i>	<i>B</i> _{iso} (Å ²)
Ti	4h	1.0	0.0	0.2795	0.5	0.35
O1	4g	1.0	0.0	0.2393	0.0	0.35
O2	4g	1.0	0.0	0.3131	0.0	0.35

^a Structural model has the *Immm* space group. *a* = 3.755 Å; *b* = 36.724 Å; *c* = 2.960(1) Å.

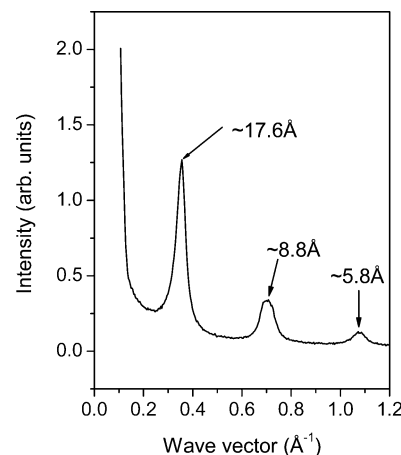


Figure 6. Experimental diffraction pattern of the product of air-dried colloidal suspension of titanate nanoparticles. The pattern shows a pronounced low-*Q* peak at ~ 17.6 Å that can be associated with the separation between the individual titanate layers building the material.

It shows a prominent low-*Q* peak corresponding to an interplanar distance of ~ 18 Å, which may be interpreted as the distance between the titanate layers in the solidified material. It is very likely that in the heavily centrifuged suspension the titanate layers are already separated at distances close to 18 Å and those distances survive when water is evaporated slowly. Previous

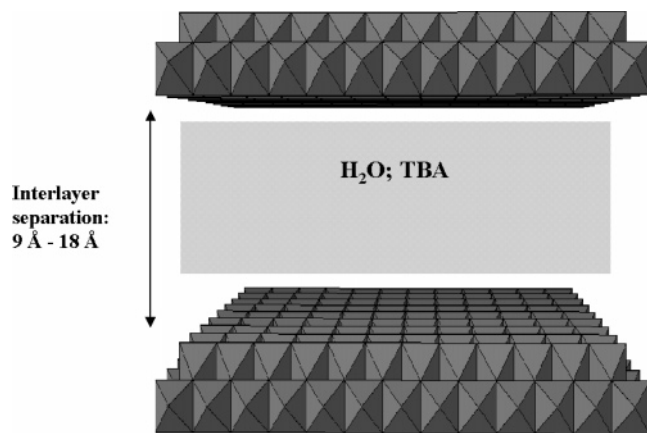


Figure 7. Schematic presentation of an exfoliated titanate nanosheet in colloidal suspension as determined by the present PDF studies.

studies by Sasaki et al.⁹ have also found that air-dried suspension of titanate sheets always shows interlayer distance of ~ 18 Å regardless of the relative concentration of water and TBA molecules in the wet material. Also, the same studies⁹ have suggested that wet titanate sheets are indeed a mixed-layer system showing interlayer distances ranging from approximately 10 to 20 Å. We checked this hypothesis by designing a model featuring titanate layers with two separations: 9 and 18 Å. The corresponding PDF is compared to the experimental data in Figure 5c. It reproduces the experimental data very well up to interatomic distances as long as 20 Å. Thus, the picture emerging from our studies is that of titanate sheets with an irregular structure. The separations between the building double layers vary from at least 9 to 18 Å as shown in Figure 7. Also, since the experimental PDF data decay to zero at approximately 20 Å, not only the correlations between the layers, but also those within the layers, are obviously short-ranged as well. This observation is consis-

tent with double layers that are either slightly bent or terminated by steps as frequently occurs with materials exhibiting Ti deficiency.²⁰

Conclusions

The 3D atomic ordering of titanate nanosheets was determined by the atomic PDF technique. Although disordered over long ranges (>20 Å⁻¹), wet titanate nanosheets is a material with substantial local order. At the atomic scale, it may be viewed as an irregular assembly of double layers of Ti–O₆ octahedra. The layers are almost uncorrelated and separated by distances of at least 1 nm with the interlayer space occupied by water molecules and organic TBA cations. The weak interaction and negligible assembling between the individual titanate layers is what makes possible the facile formation of new titanate-based heterostructures through intercalation of metal oxide/polycations and subsequent restacking. The new structural information provided by the present study, including coordinates of the atoms building the titanate nanosheets, clears the road to generating realistic structure models and performing theoretical calculations of the structure-dependent characteristics of the material. This will lead to a better understanding and, possibly, improvement of its useful properties.

Acknowledgment. Thanks to Mark Beno for the help with the synchrotron experiments. This work was supported by NSF through grant DMR 0304391(NIRT) and in part by grant R08-2003-000-10409-0 from the Basic Research Program of the Korean Science & Engineering Foundation. The Advanced Photon Source is supported by DOE under contract W-31-109-Eng-38.

CM0488884

(20) Sasaki, T.; Komatsu, Y.; Fujiki, Y. *Chem. Mater.* **1992**, *4*, 894.